Proceedings of the 2013 IEEE International Conference on
Cyber Technology in Automation, Control and Intelligent Systems
May 26-29, 2013, Nanjing, China

Frequency Control of Electric Power Microgrids Using Distributed Cooperative Control of Multi-agent Systems

Ali Bidram, Frank L. Lewis, and Ali Davoudi
The University of Texas at Arlington Research Institute and Electrical Engineering Department
The University of Texas at Arlington
ali.bidram@mavs.uta.edu, lewis@uta.edu, davoudi@uta.edu

Zhihua Qu
Department of Electrical Engineering and Computer Science
University of Central Florida
qu@eecs.ucf.edu

***Abstract*— Distributed cooperative control of multi-agent systems is used to implement the secondary frequency control of microgrids. The proposed control synchronizes the frequency of distributed generators (DG) to the nominal frequency and shares the active power among DGs based on their ratings. This frequency control is implemented through a communication network with one-way communication links, and is fully distributed such that each DG only requires its own information and the information of its neighbors on the communication network graph. Due to the distributed structure of the communication network, the requirements for a central controller and complex communication network are obviated, and the system reliability is improved. Simulation results verify the effectiveness of the proposed secondary control for a microgrid test system.**

Keywords—Distributed cooperative control, microgrids, multi-agent systems, secondary control.

I. Introduction

Microgrids are small-scale power systems that facilitate the integration of distributed generators (DG) and can operate in both gird-connected and islanded modes [1]-[6]. In normal operation, the microgrid is connected to the main grid, and its frequency is dictated by the nominal frequency of the main grid. However, the microgrid may disconnect from the main grid and goes to the islanded operation due to the pre-planned or unplanned events. Islanding process results in active power unbalance between generation and consumption units which, in turn, may cause frequency instability. The primary control is applied to maintain the frequency stability [7]-[9]. The primary control shares the active power among DGs based on their ratings. However, the primary control can lead to slight frequency deviations from the nominal frequency. To restore the DG frequencies to their nominal value, the secondary control is applied [7]-[8], [10]-[13]. The secondary control also requires sharing the active power among DGs based on their ratings. The conventional secondary controls for microgrids assume a centralized structure that requires a complex communication network [7]-[8], [10]-[11]. The requirements for a central controller and complex communication networks reduce the system reliability. Sparse communication networks can be accommodated by applying distributed cooperative control of multi-agent systems to the design of secondary control for microgrids [14].

In multi-agent systems, the coordination and synchronization process requires the exchange of information among agents based on some communication protocols [15]-[21]. A microgrid can be considered as a multi-agent system, where each DG is an agent. Since the dynamics of DGs in microgrids are nonlinear and non-identical, input-output feedback linearization can be used to transform the nonlinear heterogeneous dynamics of DGs to linear dynamics. Once input-output feedback linearization is applied, the secondary frequency control leads to a first-order synchronization problem. In this paper, fully distributed frequency control protocols are derived for each DG that synchronize the DG frequencies to the nominal value and allocate the active power of DGs based on their active power ratings. The proposed secondary frequency control is implemented through a sparse communication network. The communication network is modeled by a directed graph (digraph). Each DG requires its own information and the information of its neighbors on the digraph. The sparse communication structure requires one-way communication links and is more reliable than centralized secondary controls.

The paper is organized as follows: Section II discusses the dynamical model of inverter-based DGs and the primary and secondary control levels. In Section III, the secondary frequency control based on distributed cooperative control of multi-agent systems is presented. The proposed secondary control is verified in section IV on a microgrid test system. Section V concludes the paper.

II. Primary and Secondary Control Levels of Microgrids

Figure 1 shows the block diagram of an inverter-based DG. It contains the primary power source (e.g., photovoltaic panels), the voltage source converter (VSC), and the power, voltage, and current control loops. The control loops set and control the output voltage and frequency of the VSC. Outer voltage and inner current controller block diagrams are

This work is supported in part by the NSF under Grant Numbers ECCS-1137354 and ECCS-1128050, the AFOSR under Grant Number FA9550-09-1-0278, the ARO under Grant Number W91NF-05-1-0314, the China NNSF under Grant Number 61120106011, and China Education Ministry Project 111 (No.B08015).

elaborated in [22]. The power controller provides the voltage references v_{odi}^* and v_{oqi}^* for the voltage controller, and the operating frequency ω_i for the VSC. Note that nonlinear dynamics of each DG in a microgrid are formulated on its own *d-q* (direct-quadratic) reference frame. The reference frame of microgird is considered as the common reference frame and the dynamics of other DGs are transformed to the common reference frame. The angular frequency of this common reference frame is denoted by ω_{com}.

The nonlinear dynamics of the *i*-th DG, shown in Fig. 1, can be written as

$$\begin{cases} \dot{\mathbf{x}}_i = \mathbf{f}_i(\mathbf{x}_i) + \mathbf{k}_i(\mathbf{x}_i)\mathbf{D}_i + \mathbf{g}_i(\mathbf{x}_i)u_i \\ y_i = h_i(\mathbf{x}_i) + d_i u_i \end{cases}, \tag{1}$$

The term $\mathbf{D}_i$ is considered as a known disturbance. Detailed expressions for $\mathbf{f}_i(\mathbf{x}_i)$, $\mathbf{g}_i(\mathbf{x}_i)$, $h_i(\mathbf{x}_i)$, $d_i(\mathbf{x}_i)$, and $\mathbf{k}_i(\mathbf{x}_i)$ are adopted from the nonlinear model presented in [22].

The primary control is usually implemented as a local controller at each DG by the droop technique. Droop technique prescribes a desired relation between the frequency and the active power, and between the voltage amplitude and the reactive power. The primary frequency control is

$$\omega_i = \omega_{ni} - m_{Pi}P_i \tag{2}$$

where ω_{ni} is the primary frequency control reference and m_{Pi} is the frequency-active power droop coefficient [7]-[8].

The secondary frequency control chooses ω_{ni} such that the angular frequency of each DG synchronizes to its nominal value , i.e. $\omega_i \to \omega_{ref}$. It should be noted that once the secondary frequency control is applied, the DG output powers are allocated according to the same pattern used for primary control [23]. After applying the primary control, the DG output powers satisfy the following equality

$$m_{P1}P_1 = \cdots = m_{PN}P_N. \tag{3}$$

Since the active power droop coefficients m_{Pi} are chosen based on the active power rating of DGs, $P_{\max i}$, (3) is equivalent to

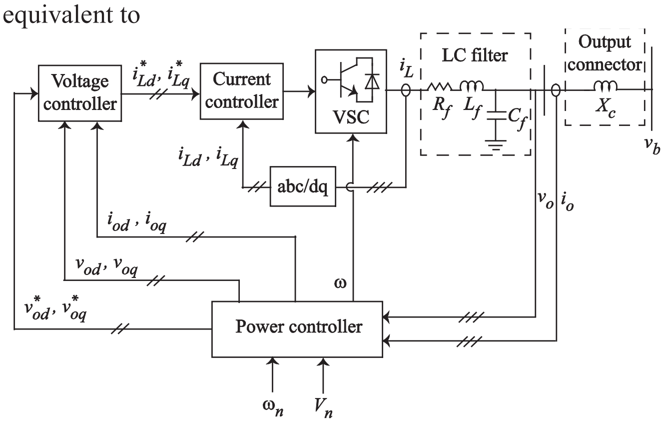

Fig. 1. The block diagram of an inverter-based DG.

$$\frac{P_1}{P_{\max 1}} = \cdots = \frac{P_N}{P_{\max N}}. \tag{4}$$

Therefore, the secondary frequency control must also satisfy (3) or (4) [23]. For the secondary frequency control, the outputs and inputs are $y_i = \omega_i$ and $u_i = \omega_{ni}$, respectively.

Conventionally, the secondary frequency control is implemented by using a centralized controller for the whole microgrid having the proportional-plus-integral (PI) structure [7]-[8]. In a centralized control structure, the central controller communicates with all DGs in the microgrid through a star communication network. A centralized control structure deteriorates the system reliability. In Section III, the distributed cooperative control of multi-agent systems will be adopted to develop a more efficient secondary frequency control with a distributed structure.

The proposed secondary frequency control exploits the following relationship between the output active power of each DG and its angular frequency. The output active power of each DG can be written as [9]

$$P_i = \frac{|v_{oi}||v_{bi}|}{X_{ci}}\sin(\delta_i) \equiv h_i \sin(\delta_i), \tag{5}$$

where δ_i is the angle of the DG reference frame with respect to the common reference frame. v_{oi} , v_{bi} , and X_{ci} are shown in Fig. 1. The term h_i can be assumed to be constant since the amplitude of v_{oi} and v_{bi} change slightly around the nominal voltage [9]. Since X_{ci} is typically small, δ_i is small, and hence, $\sin(\delta_i)$ is approximately equal to δ_i [9]. Considering these assumptions and differentiating (5) yields

$$\dot{P}_i = h_i(\omega_i - \omega_{com}), \tag{6}$$

Equation (6) provides a direct relationship between the differentiated output power of DGs and their angular frequency with respect to the angular frequency of microgrid. The global form of (6) can be written as

$$\dot{P} = h(\omega - \underline{\omega}_{com}), \tag{7}$$

where $h = diag\{h_i\}$ and $\underline{\omega}_{com} = \mathbf{1}_N \otimes \omega_{com}$.

III. Distributed Cooperative Control of Microgirds

In this section, the secondary frequency control is designed based on the distributed cooperative control of multi-agent systems. For this purpose, each DG needs to communicate with its neighbors and receive the information of neighboring DGs through one-way communication links. The required communication network can be modeled by a communication graph. In the following, first, a brief introduction on graph theory is presented. Then, the distributed cooperative secondary control of microgirds is discussed.

A. Preliminaries on Graph Theory

The communication network of a microgrid can be modeled by a digraph. In a microgrid, DGs are considered as the nodes of the communication digraph. The edges of the corresponding digraph of the communication network denote the communication links. A digraph is usually expressed as $\mathcal{G}=(\mathcal{V},\mathcal{E},\mathcal{A})$ with a nonempty finite set of N nodes $\mathcal{V}=\{v_1,v_2,\ldots,v_N\}$, a set of edges or arcs $\mathcal{E}\subset\mathcal{V}\times\mathcal{V}$, and the associated adjacency matrix $\mathcal{A}=[a_{ij}]\in\mathbb{R}^{N\times N}$. In this paper, the digraph is assumed to be time-invariant, i.e., $\mathcal{A}$ is constant. An edge from node j to node i is denoted by (v_j,v_i), which means that node j receives information from node i. a_{ij} is the weight of edge (v_j,v_i), and $a_{ij}>0$ if $(v_j,v_i)\in\mathcal{E}$, otherwise $a_{ij}=0$. It is assumed that there is no repeated edge, i.e. $a_{ii}=0$. Node j is called a neighbor of node i if $(v_j,v_i)\in\mathcal{E}$. The set of neighbors of node i is denoted as $N_i=\{j\,|\,(v_j,v_i)\in\mathcal{E}\}$. For a digraph, if node j is a neighbor of node i, then node i can receive information from node j, but not necessarily vice versa. The in-degree matrix is defined as $D=diag\{d_i\}\in\mathbb{R}^{N\times N}$ with $d_i=\sum_{j\in N_i}a_{ij}$. The Laplacian matrix is defined as $L=D-\mathcal{A}$.

A directed path from node i to node j is a sequence of edges, expressed as $\{(v_i,v_k),(v_k,v_l),\ldots,(v_m,v_j)\}$. A digraph is said to have a spanning tree, if there is a node i_r (called the root), with a directed path to every other node in the graph [24].

B. Distributed Cooperative Frequency Control

The distributed cooperative frequency control is designed to synchronize the frequency of DGs, ω_i in (2), to the reference frequency, ω_{ref}, while sharing the active power among DGs based on their power ratings as stated in (3).

The nonlinear dynamics of the i-th DG in (1) are considered. Differentiating the frequency-droop characteristic in (2) yields

$$\dot{\omega}_{ni}=\dot{\omega}_i+m_{Pi}\dot{P}_i=u_i, \tag{8}$$

where u_i is an auxiliary control to be designed. Equation (8) is a dynamic system for computing the control input ω_{ni} from u_i (See Fig. 2.). The auxiliary control should be designed such that DG frequencies synchronize to the reference frequency ω_{ref}, and (3) is satisfied. According to (8), the secondary frequency control of a microgrid including N DGs is transformed to a synchronization problem for a first-order and linear multi-agent system

$$\begin{cases}\dot{\omega}_1+m_{P1}\dot{P}_1=u_1\\ \dot{\omega}_2+m_{P2}\dot{P}_2=u_2\\ \vdots\\ \dot{\omega}_N+m_{PN}\dot{P}_N=u_N\end{cases}. \tag{9}$$

To achieve synchronization, it is assumed that DGs can communicate with each other through the prescribed communication digraph $\mathcal{G}$. The auxiliary controls u_i are chosen based on each DG's own information, and the information of its neighbors in the communication digraph as

$$\begin{aligned}u_i=-c(&\sum_{j\in N_i}a_{ij}(\omega_i-\omega_j)+g_i(\omega_i-\omega_{ref})\\&+\sum_{j\in N_i}a_{ij}(m_{Pi}P_i-m_{Pj}P_j)),\end{aligned} \tag{10}$$

where $c\in\mathbb{R}$ is the control gain. It is assumed that the pinning gain $g_i\geq 0$ is nonzero for only one DG that has the reference frequency ω_{ref}.

The global control input u is written as

$$u=-c((L+G)(\omega-\underline{\omega}_{ref})+Lm_PP), \tag{11}$$

where $\omega=[\omega_1\ \ \omega_2\ \ \cdots\ \ \omega_N]^T$, $\underline{\omega}_{ref}=\mathbf{1}_N\otimes\omega_{ref}$, with $\mathbf{1}_N$ the vector of ones with the length of N, $m_P=diag\{m_{Pi}\}$, and $P=[P_1\ \ P_2\ \ \cdots\ \ P_N]^T$. The Kronecker product is $\otimes$. $G\in\mathbb{R}^{N\times N}$ is a diagonal matrix with diagonal entries equal to the pinning gains g_i. The global form of dynamics in (9) can be written as

$$\dot{\omega}+m_P\dot{P}=-c((L+G)(\omega-\underline{\omega}_{ref})+Lm_PP). \tag{12}$$

The term $(L+G)(\omega-\underline{\omega}_{ref})$ is defined as the global neighborhood tracking error e. The term $\omega-\underline{\omega}_{ref}$ is defined as the global disagreement vector, δ.

Lemma 1 [18], [19]. Zero is a simple eigenvalue of L if and only if the directed graph has a spanning tree. Moreover, $L\mathbf{1}_N=0$, with $\mathbf{1}_N$ being the vector of ones with the length of N.

Lemma 2 [25]. Let the digraph $\mathcal{G}$ have a spanning tree and $g_i\neq 0$ for at least one root node. Then, $L+G$ is a nonsingular M-matrix. Additionally

$$\|\delta\|\leq\|e\|/\sigma_{\min}(L+G), \tag{13}$$

where $\sigma_{\min}(L+G)$ is the minimum singular value of $L+G$, and $e=0$ if and only if $\delta=0$.

In the following, it is assumed that the DG for which $g_i\neq 0$ is labeled as DG 1. Theorem 1 is the main result.

Theorem 1. Let the digraph $\mathcal{G}$ have a spanning tree and $g_i\neq 0$ for only one DG placed as a root node of digraph $\mathcal{G}$. Let the auxiliary control u_i be chosen as in (10). Then, the DG frequencies ω_i in (2) synchronize to ω_{ref}, and the active power among DGs is shared based on their power ratings satisfying (4).

Proof: In the steady state, the left sides of (12) and (7) are equal to zero. Setting the left side of (7) equal to zero yields

$$\omega = \underline{\omega}_{com}. \tag{14}$$

Equation (14) shows that all the DG frequencies synchronize to the microgrid frequency in steady state. Therefore, according to Lemma 1

$$L\omega = 0. \tag{15}$$

Setting the left side of (12) equal to zero, and considering (15) yields

$$Lm_P P + G(\omega - \underline{\omega}_{ref}) = 0. \tag{16}$$

The commensurate form of (16) can be written as

$$\begin{bmatrix} \sum\limits_{j=1:N} a_{1j} & -a_{12} & \cdots & -a_{1N} \\ -a_{21} & \sum\limits_{j=1:N} a_{2j} & \cdots & -a_{2N} \\ \vdots & \vdots & \ddots & \vdots \\ -a_{N1} & -a_{N2} & \cdots & \sum\limits_{j=1:N} a_{Nj} \end{bmatrix} \begin{bmatrix} m_{P1}P_1 \\ m_{P2}P_2 \\ \vdots \\ m_{PN}P_N \end{bmatrix} + \begin{bmatrix} g_1(\omega_1 - \omega_{ref}) \\ 0 \\ \vdots \\ 0 \end{bmatrix} = 0, \tag{17}$$

that equivalently yields (18) and (19).

$$\begin{aligned} &a_{12}(m_{P1}P_1 - m_{P2}P_2) + \cdots + a_{1N}(m_{P1}P_1 - m_{PN}P_N) \\ &+ g_1(\omega_1 - \omega_{ref}) = 0, \end{aligned} \tag{18}$$

$$(\overline{L} + \overline{G})(\begin{bmatrix} m_{P2}P_2 \\ m_{P3}P_3 \\ \vdots \\ m_{PN}P_N \end{bmatrix} - \begin{bmatrix} m_{P1}P_1 \\ m_{P1}P_1 \\ \vdots \\ m_{P1}P_1 \end{bmatrix}) = 0, \tag{19}$$

where

$$\overline{L} = \begin{bmatrix} \sum\limits_{j=1:N} a_{2j} & -a_{23} & \cdots & -a_{2N} \\ -a_{32} & \sum\limits_{j=1:N} a_{3j} & \cdots & -a_{3N} \\ \vdots & \vdots & \ddots & \vdots \\ -a_{N2} & -a_{N3} & \cdots & \sum\limits_{j=1:N} a_{Nj} \end{bmatrix}, \tag{20}$$

$$\overline{G} = \begin{bmatrix} -a_{21} & 0 & \cdots & 0 \\ 0 & -a_{31} & \cdots & 0 \\ \vdots & \vdots & \ddots & \vdots \\ 0 & 0 & \cdots & -a_{N1} \end{bmatrix}. \tag{21}$$

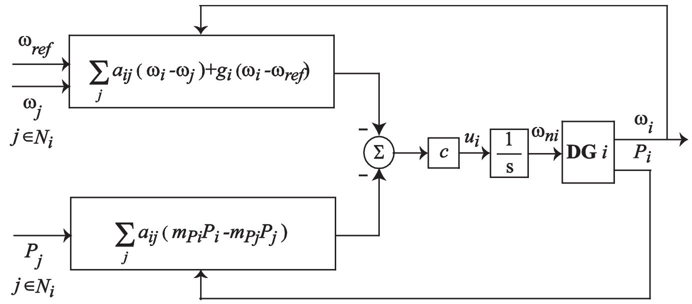

Fig. 2. The block diagram of the distributed secondary frequency control.

Equation (19) shows that the set $\{m_{P1}P_1, m_{P2}P_2, ..., m_{PN}P_N\}$ can be considered on a communication digraph with $m_{P1}P_1$ as the leader node and $m_{P2}P_2$ as the root node. All nodes have access to the leader $m_{P1}P_1$ through the matrix $\overline{G}$ in (21). Since the original digraph $\mathcal{G}$ has a spanning tree with $m_{P1}P_1$ as the root node, at least one of the diagonal terms in $\overline{G}$ is non-zero. Therefore, exploiting Lemma 2 shows that all $m_{Pi}P_i$ synchronize to a common value in the steady state which satisfies (3), or, equivalently, (4). Additionally, according to (18), having all $m_{Pi}P_i$ synchronized to a common value shows that ω_1 synchronizes to ω_{ref} and hence, according to (14), all DG frequencies synchronize to ω_{ref}. This completes the proof. □

The block diagram of the secondary frequency control based on the distributed cooperative control is shown in Fig. 2. As seen in this figure, the control input ω_{ni} is written as

$$\omega_{ni} = \int u_i dt. \tag{22}$$

C. *Sparse Efficient Communication Topology for Secondary Control*

According to Theorem 1, the communication requirements for implementing the proposed secondary control are rather mild. Specifically, the communication topology should be a graph containing a spanning tree in which the secondary control of each DG only requires information about that DG and its direct neighbors in the communication graph. Given the physical structure of the microgrid, it is not difficult to select a graph with a spanning tree that connects all DGs in an optimal fashion. Such optimal connecting graphs can be designed using operations research or assignment problem solutions [26]-[27]. The optimization criteria can include minimal lengths of the communication links, maximal use of existing communication links, minimal number of links, and so on. For microgrids with a small geographical span, the communication network can be implemented by CAN Bus and PROFIBUS communication protocols [11], [28]. It should be noted that communication links contain an intrinsic delay; however, since the time scale of the secondary control is large enough, the communication link delays do not affect the system performance [11].

TABLE I
SPECIFICATIONS OF THE MICROGRID TEST SYSTEM

DGs	DG 1 & 2 (45 kVA rating)		DG 3 & 4 (34 kVA rating)			
	m_P	9.4×10^{-5}	m_P	12.5×10^{-5}		
	n_Q	1.3×10^{-3}	n_Q	1.5×10^{-3}		
	R_c	0.03 Ω	R_c	0.03 Ω		
	L_c	0.35 mH	L_c	0.35 mH		
	R_f	0.1 Ω	R_f	0.1 Ω		
	L_f	1.35 mH	L_f	1.35 mH		
	C_f	50 μF	C_f	50 μF		
	K_{PV}	0.1	K_{PV}	0.05		
	K_{IV}	420	K_{IV}	390		
	K_{PC}	15	K_{PC}	10.5		
	K_{IC}	20000	K_{IC}	16000		
Lines	Line 1		Line 2		Line 3	
	R_{l1}	0.23 Ω	R_{l2}	0.35 Ω	R_{l3}	0.23 Ω
	L_{l1}	318 μH	L_{l2}	1847 μH	L_{l3}	318 μH
Loads	Load 1		Load 2			
	P_{L1} (per phase)	12 kW	P_{L2} (per phase)	15.3 kW		
	Q_{L1} (per phase)	12 kVAr	Q_{L2} (per phase)	7.6 kVAr		

IV. CASE STUDY

The microgrid shown in Fig. 3a is used to verify the effectiveness of the proposed secondary control. This microgrid consists of four DGs. The lines between buses are modeled as series RL branches. The specifications of the DGs, lines, and loads are summarized in Table 1. In this table, K_{PV}, K_{IV}, K_{PC}, and K_{IC} are the parameters of the voltage and current controllers in Fig. 1. The voltage and current controller parameters are adopted from [22]. The simulation results are extracted by modeling the dynamical equations of microgrid in Matlab.

It is assumed that DGs communicate with each other through the communication digraph depicted in Fig. 3b. This communication topology is chosen based on the geographical location of DGs. The associated adjacency matrix of the digraph in Fig. 4a is

$$\mathcal{A} = \begin{bmatrix} 0 & 0 & 0 & 0 \\ 1 & 0 & 0 & 0 \\ 0 & 1 & 0 & 0 \\ 0 & 0 & 1 & 0 \end{bmatrix}. \tag{23}$$

DG 1 is the only DG connected to the leader node with the pinning gain of $g_1 = 1$. The reference value for the microgrid angular frequency ω_{ref} is set as 314.16 rad/s (The nominal frequency of the microgrid is 50 Hz.). The control gain c is set to 400.

It is assumed that the microgrid is islanded form the main grid at $t = 0$. Figure 4 shows frequencies and output powers of DGs before and after applying the secondary frequency control. As seen in Fig. 4a, once the primary control is applied, DG operating frequencies all go to a common value that is the operating frequency of microgrid. However, the secondary frequency control returns the operating frequency of microgrid to its nominal value after 0.3 s. Figure 4b shows that the DG output powers all satisfy (3) and (4), and are set according to the power rating of DGs.

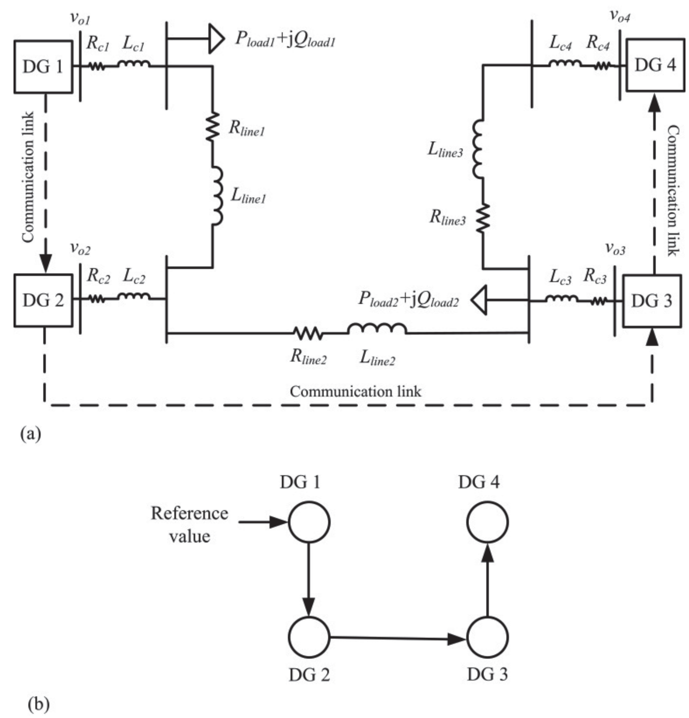

Fig. 3. (a) The microgrid test system; (b) The communication digraph.

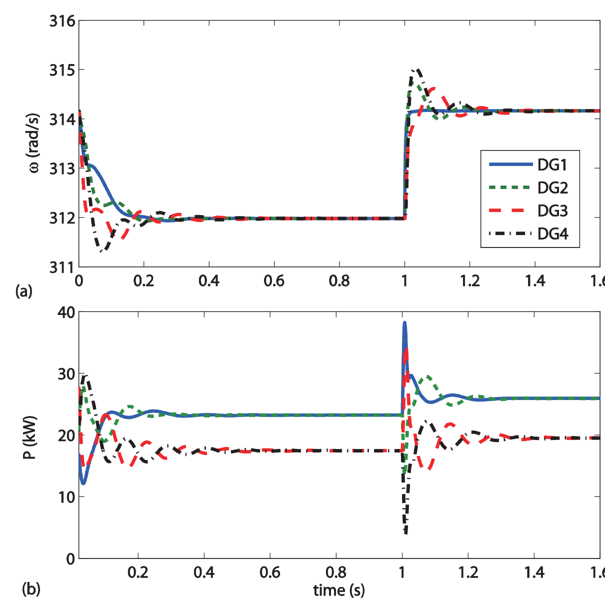

Fig. 4. The secondary frequency control with $\omega_{ref} = 314.16$ rad/s: (a) DG angular frequencies; (b) DG output powers.

V. CONCLUSION

The secondary voltage and frequency control of microgrids are designed based on the distributed cooperative control of multi-agent systems. The microgrid is considered as a multi-agent system with DGs as its agents. DGs can communicate with each other through a communication network modeled by a digraph. Input-output feedback linearization is used to transform the nonlinear dynamics of DG to linear dynamics. Feedback linearization converts the secondary voltage and frequency controls to first-order tracking synchronization problems. The control inputs are designed such that each DG only requires its own information and the information of its neighbors on the communication digraph. The proposed microgrid secondary control requires a sparse communication structure with one-way communication links and is more reliable than centralized secondary controls.

REFERENCES

[1] B. Fahimi, A. Kwasinski, A. Davoudi, R. S. Balog, and M. Kiani, "Charge it," *IEEE Power & Energy Magazine,* vol. 9, pp. 54-64, July/Aug. 2011.

[2] A. Mehrizi-sani and R. Iravani, "Online setpoint adjustment for trajectory shaping in microgrid applications," *IEEE Trans. Power Syst.,* vol. 27, pp. 216-223, Feb. 2012.

[3] A. Bidram, M. E. Hamedani-golshan, and A. Davoudi, "Capacitor design considering first swing stability of distributed generations," *IEEE Trans. Power Syst.,* vol. 27, pp. 1941-1948, Nov. 2012.

[4] A. Bidram, M. E. Hamedani-golshan, and A. Davoudi, "Loading constraints for first swing stability margin enhancement of distributed generation," *IET Generation, Transmission, and Distribution,* vol. 6, no. 12, pp. 1292-1300, 2012.

[5] R. H. Lasseter, "Microgrid," in *Proc. IEEE Power Eng. Soc. Winter Meeting*, vol. 1, New York, 2002, pp. 305-308.

[6] A. Bidram, M. E. Hamedani-golshan, and A. Davoudi, "Distributed generation placement considering first swing stability margin," *IET Electronic Letters,* vol. 48, no. 12, pp. 724-725, 2012.

[7] J. M. Guerrero, J. C. Vásquez, J. Matas, M. Castilla, L. G. d. Vicuña, and M. Castilla, "Hierarchical control of droop-controlled AC and DC microgrids-A general approach toward standardization," *IEEE Trans. Ind. Electron.,* vol. 58, pp. 158-172, Jan. 2011.

[8] A. Bidram and A. Davoudi, "Hierarchical structure of microgrids control system," *IEEE Trans. Smart Grid,* vol. 3, pp. 1963-1976, Dec. 2012.

[9] M. B. Delghavi and A. Yazdani, "A unified control strategy for electronically interfaced distributed energy resources," *IEEE Trans. Power Delivery,* vol. 27, pp. 803-812, Apr. 2012.

[10] M. D. Ilic and S. X. Liu, Hierarchical power systems control: Its value in a changing industry. London, U.K.: Springer, 1996.

[11] A. Mehrizi-Sani and R. Iravani, "Potential-function based control of a microgrid in islanded and grid-connected models," *IEEE Trans. Power Syst.,* vol. 25, pp. 1883-1891, Nov. 2010.

[12] F. Katiraei, M. R. Iravani, and P. W. Lehn, "Microgrid autonomous operation during and subsequent to islanding process," *IEEE Trans. Power Del.,* vol. 20, pp. 248-257, Jan. 2005.

[13] M. Savaghebi, A. Jalilian, J. Vasquez, and J. Guerrero, "Secondary control scheme for voltage unbalance compensation in an islanded droop-controlled microgrid," *IEEE Trans. Smart Grid,* vol. 3, pp. 797-807, June 2012.

[14] H. Xin, Z. Qu, J. Seuss, and A. Maknouninejad, "A self-organizing strategy for power flow control of photovoltaic generators in a distribution network," *IEEE Trans. Power Syst.*, vol. 26, pp. 1462-1473, Aug. 2011.

[15] Q. Hui and W. Haddad, "Distributed nonlinear control algorithms for network consensus," *Automatica*, vol. 42, pp. 2375–2381, 2008.

[16] J. Fax and R. Murray, "Information flow and cooperative control of vehicle formations," *IEEE Trans. Automatic Control*, vol. 49, pp. 1465–1476, Sept. 2004.

[17] W. Ren and R. W. Beard, Distributed consensus in multi-vehicle cooperative control. Berlin: Springer, 2008.

[18] R. Olfati-Saber and R. M. Murray, "Consensus problems in networks of agents with switching topology and time-delays," *IEEE Trans. Automatic Control*, vol. 49, pp. 1520-1533, Sept. 2004.

[19] A. Jadbabaie, J. Lin, and A. S. Morse, "Coordination of groups of mobile autonomous agents using nearest neighbor rules," *IEEE Trans. Automatic Control*, vol. 48, pp. 988–1001, June 2003.

[20] X. Li, X. Wang, and G. Chen, "Pinning a complex dynamical network to its equilibrium," *IEEE Trans. Circuits and Systems I: Regular Papers,* vol. 51, 2074–2087, Oct. 2004.

[21] Z. Li, Z. Duan, G. Chen, and L. Huang, "Consensus of multi-agent systems and synchronization of complex networks: a unified viewpoint," *IEEE Trans. Circuits and Systems I,* vol. 57, pp. 213–224, Jan. 2010.

[22] N. Pogaku, M. Prodanovic, and T. C. Green, "Modeling, analysis and testing of autonomous operation of an inverter-based microgrid," *IEEE Trans. Power Electron.*, vol. 22, pp. 613–625, March 2007.

[23] I. Serban and C. Marinescu, "Frequency control issues in microgrids with renewable energy resources," *Proc. 7th Int. Symposium on Advanced Topics in Electrical Eng.*, 2011, pp. 1–6.

[24] Z. Qu, Cooperative control of dynamical systems: Applications to autonomous vehicles. New York: Springer-Verlag, 2009.

[25] H. Zhang and F. L. Lewis, "Adaptive cooperative tracking control of higher-order nonlinear systems with unknown dynamics," *Automatica*, vol. 48, pp. 1432–1439, 2012.

[26] R. Burkard, M. Dell'Amico, and S. Martello, *Assignment Problems*. Philadelphia: SIAM: 2009.

[27] E. Bassi, F. Benzi, L. Lusetti, and G. S. Buja, "Communication protocols for electrical drives," in *Proc. 21st Int. Conf. Industrial Electronics (IECON)*, 1995, pp. 706–711.

[28] R. K. Ahuja, T. L. Magnanti, and J. B. Orlin, *Network flows: theory, algorithms, and applications*. Englewood Cliffs: Prentice Hall: 1993.